Separation Science and Technology
Publication details, including instructions for authors and subscription information:
http://www.informaworld.com/smpp/title~content=t713708471

Study of Nonsteady-State Continuous Membrane Column for Gas Separation

Zhiquan Yan[a]; Yuen-Koh Kao[a]
[a] Department of Chemical and Nuclear Engineering, University of Cincinnati, Cincinnati, Ohio

To cite this Article Yan, Zhiquan and Kao, Yuen-Koh(1988) 'Study of Nonsteady-State Continuous Membrane Column for Gas Separation', Separation Science and Technology, 23: 12, 1773 — 1788
To link to this Article: DOI: 10.1080/01496398808075662
URL: http://dx.doi.org/10.1080/01496398808075662

SEPARATION SCIENCE AND TECHNOLOGY, 23(12&13), pp. 1773-1788, 1988

STUDY OF NONSTEADY-STATE CONTINUOUS MEMBRANE COLUMN FOR GAS SEPARATION

ZHIQUAN YAN AND YUEN-KOH KAO
DEPARTMENT OF CHEMICAL AND NUCLEAR ENGINEERING
UNIVERSITY OF CINCINNATI, ML 171
CINCINNATI, OHIO 45221

ABSTRACT

The permeation and transport processes occurring in a continuous membrane column (CMC) are quite complex, and the system will exhibit inverse response behavior in a certain operating regime. To understand the complex interaction of system variables, this work developed a mathematical model for the CMC and solved the model equations. Dynamic responses of a CMC for the separation of N_2-CO_2, CO_2-O_2, and O_2-N_2 gas mixtures with capillary silicone rubber membranes are presented. The effect of the membrane permeabilities on the CMC dynamics is examined. Responses of system variables to various disturbances, together with the start-up transient of the system, are discussed. The knowledge of the unsteady-state behavior of the CMC will enable us to predict the performance of the CMC and to control the CMC in a dynamic environment.

INTRODUCTION

Membrane separation as an emerging energy-saving technique has attracted a great deal of interest. Most previous analysis of the membrane separation process, however, considered only steady state

operation (1-8). Frequently, the separation process can be treated as a steady-state process when it is operated under constant conditions or when the process disturbance is very small. However, the "dynamics" of the separation process may not be ignored when the process is operated under a dynamic environment (e.g., during startup or significant external disturbances) or under a steady dynamic (cyclic) operation. Through a detailed dynamic modeling and simulation, one can obtain a priori estimates of the system dynamics for the control system analysis and design. Unfortunately, the analysis of dynamic behavior of the membrane separation process has received little attention. Although numerous dynamic models describing the sorption and diffusion behavior of gases inside the polymer membranes exist (e.g. 9), only studies of the dynamics of a gas separation cell, using a lumped parameter model (10) and of a simple permeator, using a diffusional model (11) have been done. Thus, there is a need to study the dynamics of some practical membrane separating devices.

The Continuous Membrane Column (CMC) (12), which consists of a stripper and an enricher (see Figure 1), has recently received much attention due to its high separation efficiency and its ability to achieve very high purity products (13-18). This paper presents the findings of a computer study of dynamic responses of CMC to a variety of upsets. The dynamic model is based on the earlier model (11) of a simple permeator. Similar models can be developed for other multi-modular separation devices. The present dynamic model could be extended to include the sorption and diffusion processes inside the membrane. The extended model can be used to find ways to improve the efficiency of gas separation by membrane permeation under dynamic operations (19).

DYNAMIC MODEL AND SIMULATION METHOD

Since CMC consists of two simple permeators, an enricher and a stripper (see Figure 1), the model employed here is almost identical to that of Kao and Yan (11), except that the two permeators are connected. The major assumptions in deriving the model are that the binary gas mixture can be viewed as Newtonian, ideal gas in axial laminar flow which obeys the Poiseuille velocity distribution, and that the dynamics within the thin membrane are negligible. The Quasi-Steady-State Assumption is used to overcome the stiffness of the problem (11). It assumes that, as compared to the composition change, the changes in the gas velocity and pressure are so fast that they can be considered to occur instantaneously.

For the purpose of identifying the system parameters, the variables are made dimensionless by defining $q_t^* = q_t/f_0$; $q_s^* = q_s/f_0$; $P_t^* = P_t/P_c$; $P_s^* = P_s/P_c$; $z^* = z/L$; $t^* = t/t_0$, where f_0 is the maximum permeation rate across the membrane, $f_0 = A_m P_c Q_1/(r_o - r_i)$, and t_0 is the residence time of the tube side based on this maximum

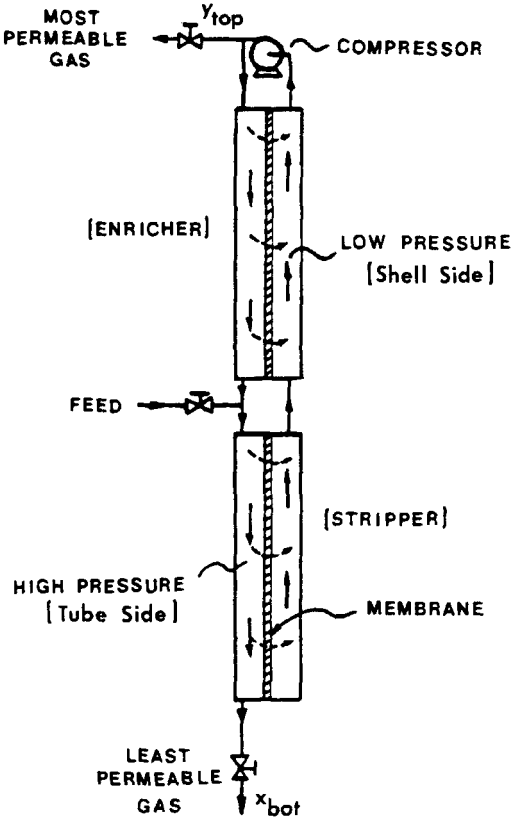

Fig. 1 Continuous Membrane Column

permeation rate, $t_0 = A_t$ TL $P_c/(f_0 RT)$. The model equations based on the above demensionless variables are listed in Table 1. The boundary conditions for the above equations, as listed in table 2, are identical to those for stand-alone stripper and enricher (11). Only the junction relations between the stripper and the enricher around the feed points need to be modified. The system is determined by six dimensionless parameters which are listed in table 3. The orthogonal collocation method is used to reduce the partial differential equations of the model to sets of ordinary differential equations (see 11 for details). For cases where the internal flow rate is high, the insignificant tube-side diffusion term in the model is ignored. The computations were performed on an AMDAHL 470.

Table 1. Dynamic Equations of the Model

$$\frac{\partial x}{\partial t^*} = \frac{1}{P_t^* \xi^j}\left[\frac{\partial (x q_t^*)}{\partial z^*} - \xi^j (x P_t^* - y P_s^*) + \alpha_2{}^j \frac{\partial^2 x}{\partial z^{*2}}\right]$$

$$\frac{\partial y}{\partial t^*} = \frac{1}{r_y \xi^j}\left[-\frac{\partial (y q_s^*)}{\partial z^*} + \xi^j (x P_t^* - y P_s^*) + \alpha_1{}^j \frac{\partial^2 y}{\partial z^{*2}}\right]$$

$$\frac{dq_s^*}{dz^*} = \xi^j \left[(x P_t^* - y P_s^*) + \frac{1}{\gamma}\left[(1-x) P_t^* - (1-y) P_s^*\right]\right]$$

$$0 = \frac{dP_t^*}{dz_*} - \beta^j \frac{q_t^*}{P_t^*}$$

$$0 = \frac{dq_t^*}{dz^*} - \frac{dq_s^*}{dz^*}$$

where j = s for stripper and e for enricher.

Table 2. Boundary Conditions of the Model

STRIPPER	ENRICHER
$\frac{dy}{dz^*}(1) = 0$	$\frac{dy}{dz^*}(1) = 0$
$\frac{dy}{dz^*}(0) = 0$	$q_s^{*s}(1) y^s(1) = q_s^{*e}(0) y^e(0) + \alpha_1 \frac{dy^e}{dz^*}(0)$
$\frac{dx}{dz^*}(0) = 0$	$\frac{dx}{dz^*}(0) = 0$
$q_F^* x_F + q_t^{*e}(0) x^e(0) = q_t^{*s}(1) x^s(1) + \alpha_2 \frac{dx^s}{dz^*}(1)$	$q_t^{*e}(1) y^e(1) = q_t^{*e}(1) x^e(1) + \alpha_2 \frac{dx^e}{dz^*}(1)$
$q_t^{*s}(1) = q_F^* + q_t^{*e}(0)$	$q_t^{*e}(1) = q_s^{*e}(1) - q_{top}^*$
$q_s^*(0) = 0$	$q_s^{*e}(0) = q_s^{*s}(1)$
$P_t^{*s}(1) = P_t^{*e}(0)$	$P_t^{*e}(1) = P_c$

Table 3. Dimensionless parameters

$\gamma = Q_1/Q_2$	perm-selectivity
$\tau_y = \frac{A_s P_s}{A_t P_c}$	time constant
$\alpha_1^j = \frac{D_0 A_s P_s}{L^j f_0 RT}$	reciprocal of shell-side Peclet number
$\alpha_2^j = \frac{D_0 A_t P_s}{L^j f_0 RT}$	reciprocal of tube-side Peclet number
$\beta^j = \frac{8\pi\mu RT f_0 L^j}{A_t r_i^2 P_c^2}$	pressure-drop coefficient
$\xi^j = L^j / TL$	column length ratio

where j = s for stripper and e for enricher.

SIMULATION RESULTS AND DISCUSSIONS

The separations of CO_2-N_2, CO_2-O_2 and O_2-N_2 gas systems are simulated with the operating conditions and the parameters, as listed in Table 4, taken from the previous experimental work (13).

The model's accuracy is verified by comparing the steady-state solution via the dynamic models with the steady-state experimental data. To this end, the dynamic simulation of the column under the changes in operating conditions from case 1 to case 2, as listed in Table 4, is made. Figure 2 shows the composition profiles of both the initial and final steady state. Both profiles are in excellent agreement with the experimental data.

Step Responses for Various Disturbances

In order to estimate the sensitivities and the dynamic behavior of the column to various disturbances, a number of step changes in operating conditions from the initial steady state (listed as case 3) was made. Figure 3 shows the initial steady state concentration profiles. The initial steady-state values for x_{bot}, y_{top}, and the dimensionless compressor load are 0.1524, 0.2901 and 0.3365 respectively.

Table 4. Operating conditions for the CMC simulations

Operating conditions	O_2-N_2 case 1	O_2-N_2 case 2	O_2-N_2 case 3	CO_2-N_2 case 4	CO_2-O_2 case 5
Feed composition	0.210	0.209	0.217	0.548	0.572
Feed flow rate (μmol/s)	6.13	13.85	7.42	10.60	14.64
Top product rate (μmol/s)	1.79	0.933	3.34	4.83	7.90
Compressor pressure (kPa)	230.14	227.34	225.62	226.62	224.85
Shell-side pressure (kPa)	101.22	98.59	98.79	99.27	99.07
Temperature (K)	296.3	297.1	299.5	298.5	298.7
Enricher length (m)	2.13	2.13	3.11	3.11	3.11
Stripper length (m)	2.11	2.11	2.01	2.01	2.01

35 silicone rubber capillaries:ID=0.235mm,OD=0.61mm. Permeabilities (mole.m.sec^{-1}m^{2}Pa^{-1}): CO_2:82.9x10^{-14}; O_2:16.8x10^{-14}; N_2:8.75x10^{-14}.

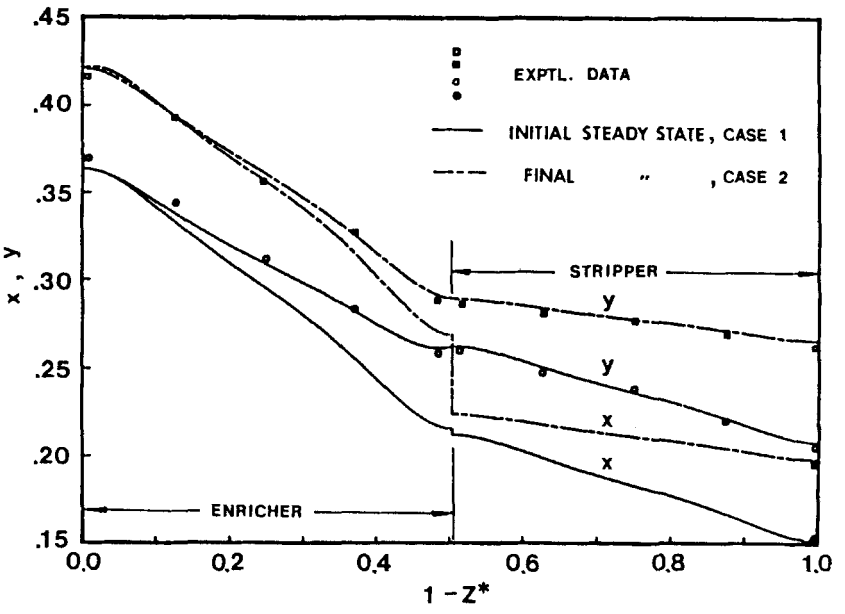

Fig. 2. Comparison of Steady State Composition Profiles in a CMC Before and After the Simultaneous Changes in Operating Conditions

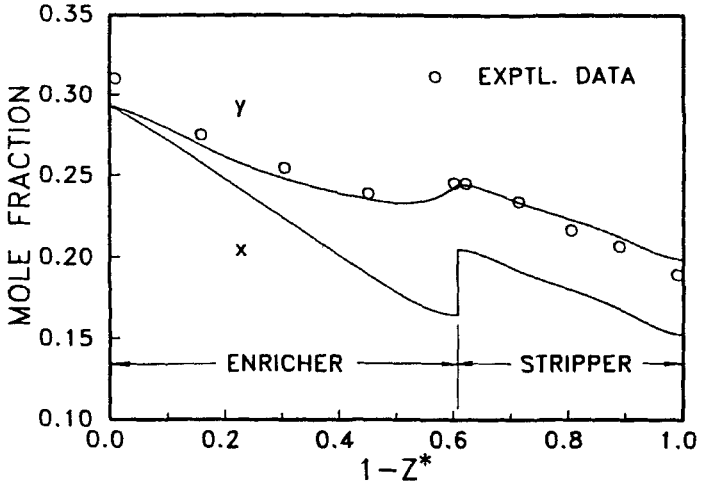

Fig. 3. Steady-state composition profiles of case 3 before step disturbances

Feed flow rate step response. Figure 4a shows the responses of the top and the bottom product compositions, y_{top} and x_{bot}, when the feed flow rate is subject to a 5% increase. It shows that x_{bot} responds faster than y_{top} due partly to the differences in time constants of the tube- and shell-side compositions (τ_y=11 for the case studied). A significant delay of about 30 residence times is observed in y_{top} response. This delay is caused by the slow gas permeation process through the membrane, which is situated between the feed disturbance and the response variable, y_{top}. The x_{bot} response shows a very sharp initial increase with the increase in feed rate, followed by a period of more gradual increase, while y_{top} shows a very slight decrease initially and then an increase towards its final steady-state value. This inverse response behavior of y_{top} is a unique feature of enricher dynamics (11). The complex response sequence can best be understood by following the compressor load (defined as the top flow rate in the shell side of the enricher) change, which is also shown in Figure 4a. The compressor load shows an initial decrease as the result of the momentary lowering of the tube-side pressure, which is caused by the sudden flow rate increase on the tube-side of the stripper; a period of rapid increase follows. This increase is due to the increase in the driving force, a result of the increase in the tube-side concentration of the more permeable species. The increasing permeation rate will cause a buildup of the more permeable species in the shell side. This will eventually cause

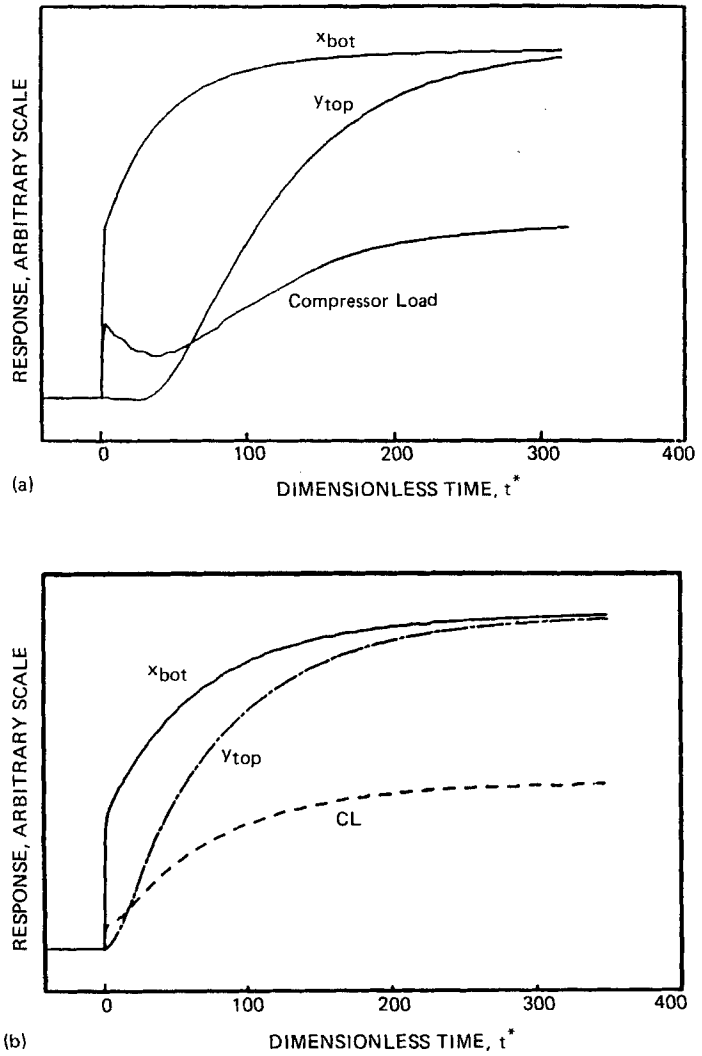

Fig. 4. Step Responses of Top and Bottom Variables To a) a Feed Flow Rate Change; b) Top Product Flow Rate Change; c) Compressor Pressure Change; d) Feed Composition Change in a CMC

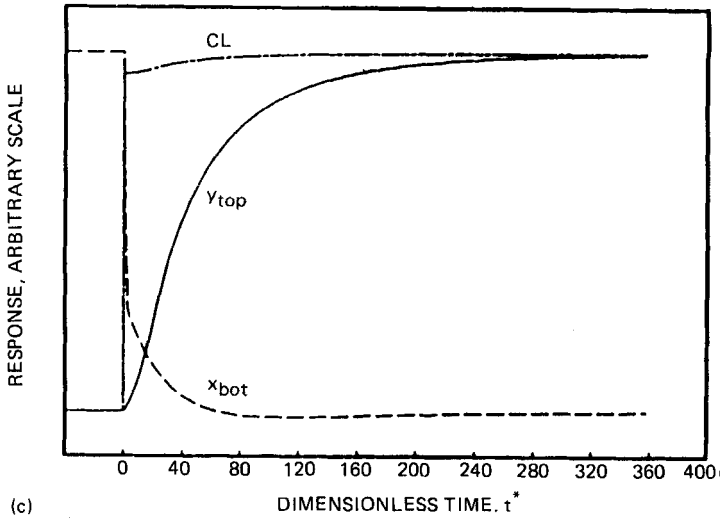

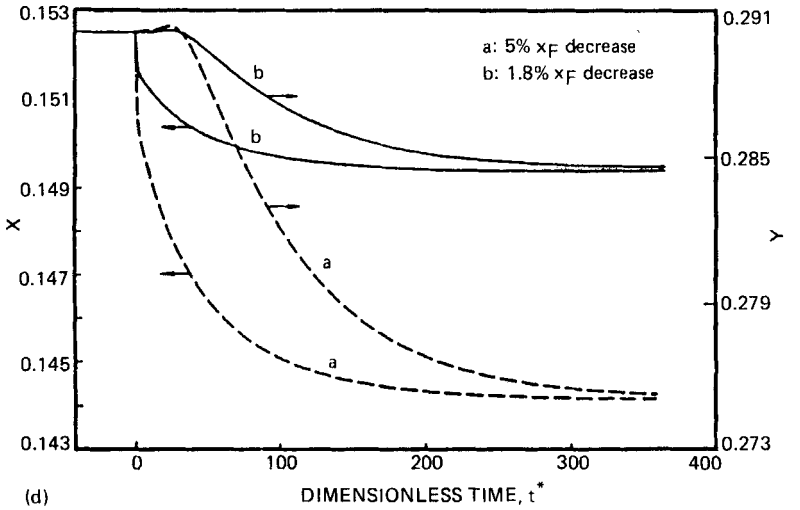

FIG. 4 continued

the permeation rate to decrease. The final value of y_{top} is higher than the initial value due to the fact that the initial feed rate is so low that the enricher is inefficiently operated, as indicated by the existance of a minimum in the initial enricher concentration profile (see Figure 3). Reverse permeation (from shell to tube side) takes place in the region where the concentration decreases along the flow direction. The increase in the feed rate will make the enricher operate more efficiently. This results in the final period of increasing permeation rate before the CMC reaches the new steady state.

Top product flow rate step response. Figure 4b shows the transient behavior of y_{top} and x_{bot} to a 5% decrease in the top product flow rate. This change, which is equivalent to a feed rate increase, will also result in a final increase in the top product composition. The transient behavior is similar to the case of feed rate step response. However, the delay in y_{top} response is absent. This is because the change in the top product rate affects flow rates and compositions on both sides of the membrane. This effect results in an immediate increase in the permeation rate (or compressor load) in the enricher. Due to the very short transfer path from the disturbance to the top product stream, y_{top} responds instantaneously to the top product rate change.

Compressor pressure step response. The responses of y_{top}, x_{bot} and the compressor load to a 5% increase in the compressor pressure are shown in Figure 4c. Since a higher tube-side pressure will improve the separation efficiency of the column, the top product composition increases and the bottom product composition decreases. The response speed of y_{top} is slower than that of x_{bot}, as previously stated, due to the slow membrane permeation process which controls the y_{top} response. The compressor load response shows an instantaneous increase due to the sharp initial increase in the permeation rate caused by the pressure increase in the tube side; the instantaneous increase is followed by a period of gradual increase as the result of the concentration changes on either side of the membrane.

Feed composition step response. The responses of y_{top} and x_{bot} to a 5% feed composition decrease are shown in Figure 4d. The delay in the y_{top} response, as in the case of feed rate change, is due to the locations of the disturbance and the response variable. It is obvious that the decrease in feed composition results in a general lowering of the composition profiles in CMC, resulting in a decrease in the permeation driving force. As was observed earlier in the feed rate step response, the bottom product composition responds faster than the top product concentration to the composition change due to the location of the disturbance.

Also shown in Figure 4d are the dynamic responses of the product compositions to a -1.8% step change in feed composition. The comparisons of the responses of x_{bot} and y_{top} to different step

Table 5. Relative Gain[a] and Time Constants of Step Responses

Disturbances	Relative Gain			Time Constant	
	x_{bot}	y_{top}	Compressor load	x_{bot}	y_{top}
+5% Feed flow rate change	0.472	0.166	0.024	42	95
-5% Feed composition change	1.089	1.034	0.166	43	90
-1.8% Feed composition change	1.094	1.053	0.165	42	90
-5% Top product rate change	-0.210	-0.448	-0.071	62	80
+5% Top pressure change	-0.761	0.724	1.920	22	50

[a] the ratio of percentage change of output variable to that of disturbance.

changes show similar dynamic behaviors. This suggests that the system behaves linearly in the domain of small perturbations.

Comparison of transient response to various step disturbances. Table 5 summarizes the relative gains of the output variables (y_{top}, x_{bot}, and the compressor load) to different disturbances. It shows that the product compositions (x_{bot}, y_{top}) are more sensitive to the changes in compressor pressure and in the feed composition and are less sensitive to the feed flow rate change, due to the large reflux stream. Feed flow rate has a moderate effect on the bottom product composition, while the top product rate has a moderate effect on the top product composition. The feed flow rate change is responsible for the sharp initial transient in all the x_{bot} responses (about 3 dimensionless times). Also observed is a delay of about 30 dimensionless times in y_{top} responses to the changes in feed conditions, but this delay is nearly absent in the responses to changes in operating condition at the top of the column. The remainder of the transients in y_{top} and x_{bot} is dominated by the same slow membrane permeation process and has the appearance of a first-order system. The time constant, identified as the time when the response reaches 63.2% of its total change (disregarding the sharp initial change in x_{bot}), is also listed in table 5. Table 5 shows that the dynamics of the product compositions to either feed composition or flow rate change can be characterized by the same time constant, but different time constants are required to characterize the product composition responses to the changes in the top product rate and in the compressor pressure, respectively.

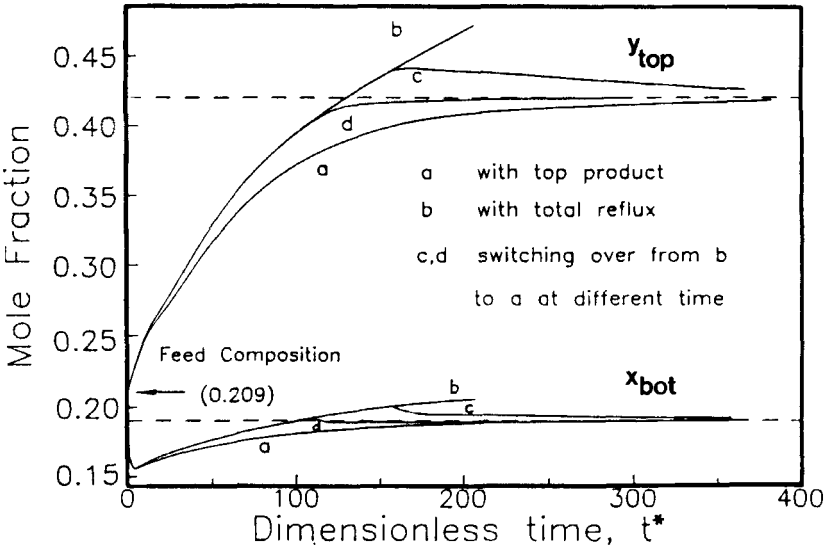

Fig. 5. Start-up transient responses of Top and Bottom Product Compositions in a CMC

Start-Up Operation

The start-up of a CMC for the O_2-N_2 system to reach the steady state operating condition, listed as case 2, is simulated. The initial composition profiles on both sides of the membrane are uniform at the feed composition. Figure 5 shows the responses of the top and the bottom compositions under two different start-up strategies. In the first strategy, the top product is withdrawn from the beginning. In the second strategy, the column is operated initially at total reflux and then switched over to the top product withdrawal at the target rate when y_{top} is brought near to the desired steady-state. Since a CMC operating at the total reflux condition will achieve the highest steady-state permeate concentration, the time required for y_{top} to reach the desired steady state value will be the least. The time required for CMC to reach the normal operation with an initial total reflux strategy is about 120 residence times, while start-up time is doubled when the column is operated with top product withdrawal from the beginning of the operation.

Figure 5 also shows that y_{top} increases steadily during the start-up period while x_{bot} decreases sharply initially and then increases towards its steady-state value. This inverse response is

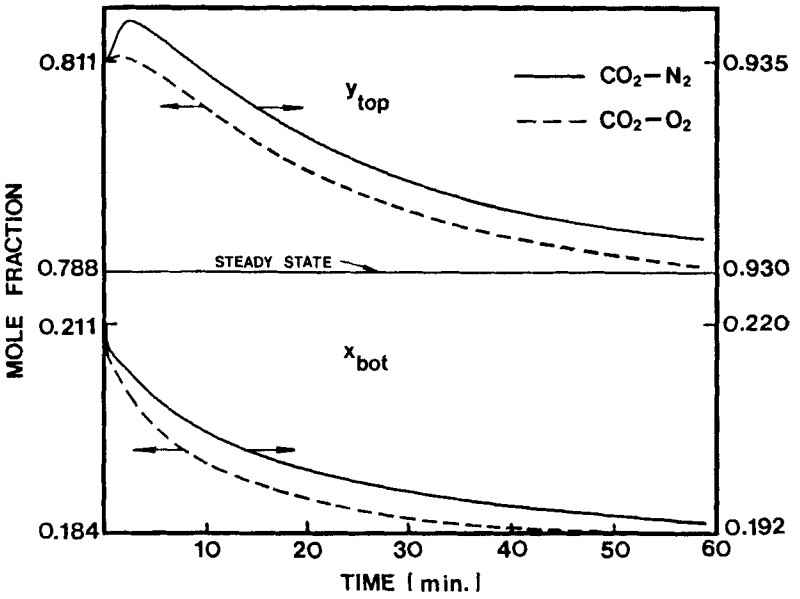

Fig. 6 Comparison of step responses of top and bottom product compositions to a feed flow rate change for different gas systems in a CMC

typical for a countercurrent process (11). The sharp drop in x_{bot} is due to the very large permeation rate at the beginning of the operation when the tube- and shell-side compositions are close. The accumulation in the shell side and the depletion in the tube side of the more permeable species will reduce, and even reverse, the direction of the permeation flux.

Effect of Selectivity On the CMC Dynamics

Among the dimensionless parameters listed in table 3, the one that affects the steady-state performance of the CMC the most is the perm-selectivity. A membrane with a greater selectivity for the gas mixture provides a larger product separation in a column at a given membrane area, and the same product separation can be achieved for the gas mixture in a smaller column with a membrane of greater selectivity. The effect of selectivity on the CMC dynamics is examined with two different gas systems, CO_2-N_2 (case 4) and CO_2-O_2 (case 5), with selectivities of 10 and 5 respectively. Their dynamic responses to the 5% decrease in feed flow rate is shown in Figure 6. Both system responses show a similar behavior. As the feed rate decreases, the stripper feed composition increases

slightly due to the lower composition of the recycle stream from the enricher. Both y_{top} and the permeation rate show an initial increase due to the enricher's inverse response behavior. After the tube-side composition profiles are lowered, both x_{bot} and y_{top} start to decrease until their final steady states are reached. The fact that the CO_2-O_2 system has faster responses for both product compositions than the CO_2-N_2 system responses is due to the larger total permeation rate of the former system. The relatively larger actual disturbance in feed rate to the CO_2-O_2 system (due to its higher initial feed rate) leads to greater ultimate changes in the product compositions.

SUMMARY

CMC is more sensitive to the step changes in compressor pressure and in feed composition than to the changes in feed flow rate. Top product concentration dynamics exhibit an inverse response behavior in certain operating regimes. Top product composition has a delay in responding to the change in feed conditions. The start-up time can be significantly reduced by operating the CMC initially at total reflux and then switching over, at an optimal time, to the normal operation with product withdrawl. The present work on the dynamics of CMC could be extended to other similar separation devices. The dynamics model can also be used to study the operation of the membrane separation devices under steady dynamic (cyclic) mode.

NOMENCLATURE

A_t, A_s	tube- or shell-side cross-sectional area, m^2
A_m	total membrane area, m^2
D_0	diffusivity, m^2/sec
L,TL	length of the permeator and the total length of the column,m
P	pressure, Pa
Pc	pressure at compressor, Pa
P_0	standard pressure, Pa
Q_1, Q_2	permeability of more or less permeable species, $mole.m/sec.m^2.Pa$
q	flow rate, mole/sec
r_i, r_o	inside and outside radius of membrane capillary, m
t	time, sec
x	tube-side composition, mole fraction of more permeable component
y	shell-side composition, mole fraction of more permeable component
z	the distance from the bottom of each permeator, m

Greek Symbols

see Table 3.

Subscripts

bot	values at bottom
F	feed stream
s	shell side
t	tube side
top	values at top

Superscripts

*	dimensionless
s,e	stripper and enricher, respectively

REFERENCES

1. S.L. Matson, J. Lopez and J.A. Quinn, Separation of gases with synthetic membranes. Review article No. 13, Chem. Eng. Sci., 38,503 (1983)

2. Z. Yan, and Y.K. Kao, Comparative study of two-membrane permeators for gas separations, paper presented in AIChE 1987 Annual Meeting, New York, NY (1987)

3. Y.K. Kao, S. Chen and S.T. Hwang, A comparative study of membrane separator designs, to appear in Membrane Technology Review (1987)

4. F.P. McCandless, A comparison of some recycle permeators for gas separations, J. Memb. Sci., 24, 15 (1985)

5. J.E. Perrin and S.A. Stern, Modeling of permeators with two different types of polymer membranes, AIChE J. 31,1167 (1985)

6. A. Sengupta and K.K. Sirkar, Ternary gas mixture separation in two-membrane permeators, AIChE J., 33, 529 (1987)

7. D.R. Seok, S.G. Kang, and S.T. Hwang, Separation of Helium and hydrocarbon mixtures by a two-membrane column. J. Memb. Sci., 27, 1 (1986)

8. J.E. Perrin and S.A. Stern, Separation of a Helium-Methane mixture in permeators with two different types of polymer membranes, AIChE J., 32,1889 (1986)

9. P. Masi, and D. R. Paul, Modeling Gas Transport In Packing Applications, J. Memb. Sci., 12, 137 (1982)

10. K.K. Koh, K. Kammermeyer, and S.T. Hwang, Frequency response characteristics of flow of gas through porous media, Chem. Eng. Sci., 24, 1191 (1969)

11. Y.K. Kao and Z. Yan, Dynamic modeling and simulation of simple membrane permeators, Chem. Eng. Comm., 59, 343 (1987)

12. S.T. Hwang, and J.M. Thorman, The Continuous Membrane Column, AIChE J., 26, 558 (1980)

13. J.M. Thorman, and S.T. Hwang, Engineering Aspects of the Continuous Membrane Column, Amer. Chem. Soc. Symp. Ser., 154, 259 (1981)

14. S.T. Hwang, and K. H. Yuen, Gas Separation by a Continuous Membrane Column, Sep. Sci. Technol., 15 (4), 1069 (1980)

15. R.A. Yoshisato, and S.T. Hwang, Computer Simulation of A Continuous Membrane Column, J. Memb. Sci., 18, 241 (1984)

16. S.T. Hwang, and S. Ghalchi, Methane Separation by a Continuous Membrane Column, J. Memb. Sci., 11, 187 (1982)

17. S. Chen, Y.K. Kao, and S.T. Hwang, A Continuous membrane column model incorporating Axial diffusion terms, J.Memb.Sci,26,143,1986

18. H.K. Lonsdale, The Growth of Membrane Technology, J. Memb. Sci., 10, 81 (1982)

19. D.R. Paul, Membrane Separation of Gases Using Steady Cyclic Operation, Ind. Eng. Chem. Proc. Des. Dev., 10, 375 (1971)